PROCEEDINGS OF SCIENCE

Measurements of net-proton fluctuation for p+p collisions at $\sqrt{s} = 200$ GeV from the STAR experiment

Risa Nishitani for the STAR Collaboration*
University of Tsukuba, Tomonaga Center for the History of the Universe
E-mail: s2312412@gmail.com

Understanding a QCD phase structure is one of the ultimate goals of heavy-ion collision experiments. Recent publications from the STAR Collaboration show a non-monotonic energy dependence of fourth-order fluctuations of net-proton, which could indicate a possible signature of the critical point at $\sqrt{s_{\mathrm{NN}}} \approx 7.7$ GeV. The sixth-order fluctuations of net-proton multiplicity distributions were reported to be negative for central Au+Au collisions at $\sqrt{s_{\mathrm{NN}}} = 200$ GeV. This could suggest a smooth crossover transition at top RHIC energy. In this paper, we present the results of higher-order fluctuations of net-proton up to the sixth-order from p+p collisions at $\sqrt{s} = 200$ GeV. It provides precise physics baselines to be compared to Au+Au collisions. The positive signs of the fifth- and sixth-order fluctuations in p+p collisions are observed and their multiplicity dependences are found to connect smoothly to those from Au+Au collisions.

CPOD2021 - the International conference on Critical Point and Onset of Deconfinement
15 - 19 March 2021
Zoom

*Speaker.

1. Introduction

The QCD phase diagram is characterized by temperature (T) and baryon chemical potential (μ_B). There is a phase of hadron gas in the region of low T and μ_B, while the phase of Quark-Gluon Plasma is expected in the high T and/or μ_B region. On the other hand, the phase transition between these two phases is still very uncertain. The phase transition at $\mu_B = 0$ is shown to be a smooth crossover by lattice QCD calculations [1], while at large μ_B, model calculations predict the first-order phase transition [2]. If the latter is true, the QCD critical point should exist, which is a connecting point between the smooth crossover and first-order transition.

In order to study the phase structure, the Beam Energy Scan program has been performed at RHIC at various collision energies for $7.7 \leq \sqrt{s_{NN}}$ (GeV) ≤ 200. The fourth-order fluctuations of net-proton multiplicity distributions show non-monotonic beam energy dependence for Au+Au central collisions [3,4], which is qualitatively similar to the theoretical model prediction incorporating the critical point [5]. Thus, the results could indicate a possible signature of the critical point. Further, the fifth- and sixth-order fluctuations have been also measured. The observed negative signs in central Au+Au collisions at $\sqrt{s_{NN}}$ = 200 GeV [7] could be a signature of smooth crossover at RHIC top energy [6, 8].

In this paper, rapidity (y) acceptance dependence of higher-order fluctuations of net-proton multiplicity distributions are measured for p+p collisions at $\sqrt{s}$ = 200 GeV. The multiplicity dependence is compared to those from Au+Au collisions.

2. Cumulant

The nth-order cumulant (C_n) is expressed as $C_1 = \langle N \rangle$, $C_2 = \langle (\delta N)^2 \rangle$, $C_3 = \langle (\delta N)^3 \rangle$, $C_4 = \langle (\delta N)^4 - 3\langle (\delta N)^2 \rangle \rangle^2$ with $\langle \delta N \rangle = N - \langle N \rangle$, where the bracket represents the average over events. Further higher-order cumulants can be also defined in similar way [9]. In this analysis we measure cumulant ratios, C_2/C_1, C_3/C_2, C_4/C_2, C_5/C_1, and C_6/C_2 to cancel the trivial volume dependence in the cumulants. Neutrons cannot be measured in the STAR experiment, and therefore the net-proton number is measured as a proxy of net-baryon. If protons and antiprotons follow independent Poisson distributions, the resulting net-proton distribution follows the Skellam distribution. The Skellam baselines are defined as unity for C_4/C_2, C_5/C_1, and C_6/C_2.

3. Data set

In this analysis, 220 million events of p+p collisions at $\sqrt{s}$ = 200 GeV taken in 2012 are analyzed in the kinematic region of $|y| < 0.5$ and $0.4 < p_T$ (GeV/c)< 2.0. The events are required to have the collision vertex within 30 cm from the center of the detectors and 2 cm for the radial directions, respectively. Collision pileups are reduced by requiring the difference of measured vertex positions along the beam direction between Vertex Position Detector and Time Projection Chamber (TPC) to be less than 3 cm. The distance of closest approach is required to be less than 1 cm in order to suppress secondary particles, and at least 20 hits in the TPC are required. Identifications of protons and anti-protons are mainly based on the energy loss (dE/dx) in the TPC for $0.4 < p_T$ (GeV/c)< 0.8. Since different particle species in the dE/dx are merged each other at high momentum region, mass squared given by Time of flight (TOF) is used at $0.8 < p_{\mathrm{T}}$ (GeV/c)$<$ 2.0.

4. Analysis method

Several corrections are applied to consider effects from various experimental artifacts. Measured cumulants are corrected for detector efficiencies assuming that detector responses follow binomial model [9–16]. Multiplicity and p_{T} dependence of efficiencies are taken into account. Centrality bin width correction (CBWC) is applied to suppress the initial volume fluctuations [17, 18]. The multiplicity is defined by charged particles excluding protons and anti-protons to suppress the auto-correlations. Statistical errors are estimated by bootstrap method [15, 18].

5. Results

Figure 1 shows the multiplicity dependence of net-proton cumulants. Results from CBWC are shown at the average of charged particle multiplicity. The Skellam baselines and PYTHIA 8 calculations are shown in dotted lines and bands, respectively. The PYTHIA 8 calculations are performed by 80 million events. It is found that cumulants increase as the multiplicity increases,

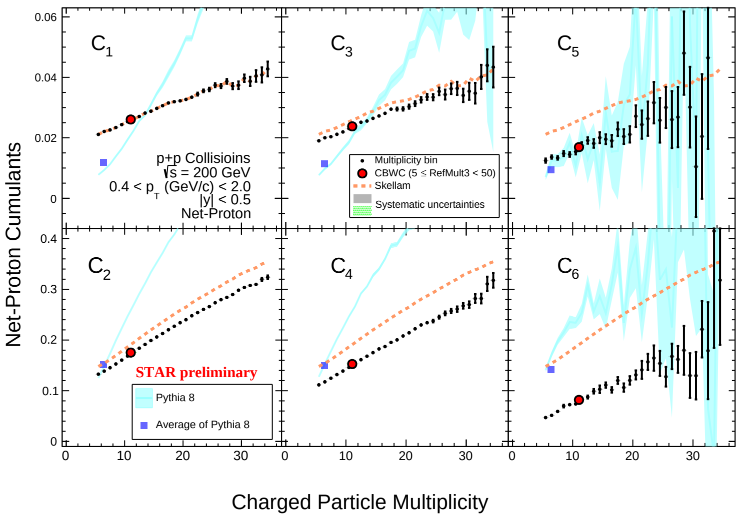

Figure 1: Net-proton cumulants up to the sixth-order as a function of multiplicity in p+p collisions at $\sqrt{s} = 200$ GeV. Red points represent the average over the multiplicity region from 5 to 50. The error bars are statistical and bands are systematic errors. The uncertainties for averaged cumulants are smaller than the marker size. The Skellam expectations are shown in dotted lines. PYTHIA 8 calculations are shown as light blue bands.

which is obvious from the trivial volume dependence of cumulants. There are large deviations at higher-orders from the Skellam baseline. Deviations from PYTHIA 8 calculations are also seen except for C_5. The multiplicity dependence of cumulant ratios is shown in Fig. 2. The multiplicity

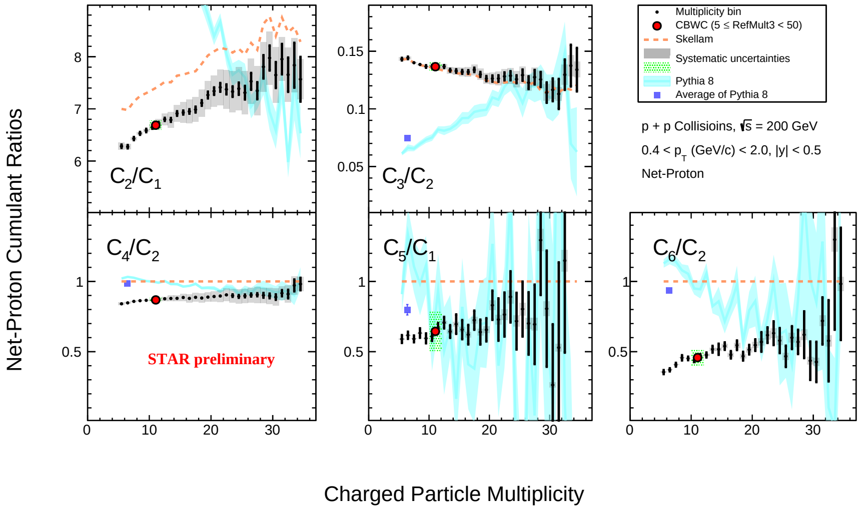

Figure 2: Net-proton cumulant ratios as a function of multiplicity for p+p collisions at $\sqrt{s} = 200$ GeV. Red points represent the average over the multiplicity region from 5 to 50. The error bars are statistical and bands are systematic errors. The uncertainties for averaged cumulants are smaller than the marker size. The Skellam expectations are shown in red lines. PYTHIA 8 calculations are shown as right blue bands.

dependence and CBWC results are compared with the Skellam baseline and PYTHIA 8 calculations. The ratios mostly deviate from the Skellam baselines except for C_3/C_2, which would be due to the comparable deviation in C_2 and C_3. Results are quite different between the data and PYTHIA 8 calculations, especially at low multiplicity region.

Rapidity acceptance dependence of CBWC results for the cumulant ratios is shown in Fig. 3. It can be seen that the results are different from Skellam expectations except for C_3/C_2 as discussed in Fig. 2. It is found that the results decrease with increasing the rapidity acceptance. Larger deviations are observed for higher-order cumulant ratios.

Figure 4 shows the multiplicity dependence of C_4/C_2, C_5/C_1, and C_6/C_2, where the results from Au+Au collisions at $\sqrt{s_{\rm NN}} = 200$ GeV are overlaid on top of the results from p+p collisions. Results from hadron resonance gas model, PYTHIA 8, lattice QCD, and the Skellam expectations are also shown. PYTHIA 8 and Skellam expectations are closer to the values of p+p than those of Au+Au central collisions. It is found that $C_4/C_2 > C_5/C_1 > C_6/C_2$, which is qualitatively consistent with the hierarchy observed in lattice QCD calculations [6, 8]. Positive signs of C_5/C_1 and C_6/C_2 are observed for p+p collisions for the entire multiplicity region. In Au+Au collisions, on the other hand, C_6/C_2 values become progressively negative from peripheral to central collisions. The observed negative sign is qualitatively consistent with lattice QCD calculations. The lattice calculations imply chiral phase transition in the thermalized QCD matter. Our measurements could indicate that the scenario applies to Au+Au central collisions at $\sqrt{s_{\rm NN}} = 200$ GeV, while not to p+p collisions.

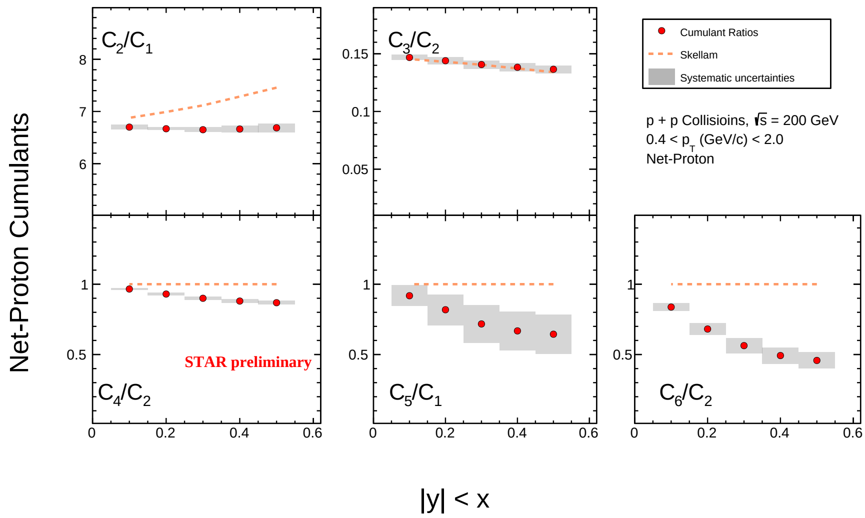

Figure 3: Net-proton cumulant ratios as a function of rapidity acceptance for *p+p* collisions at $\sqrt{s}$ = 200 GeV. Red circles represent the average over the multiplicity region from 5 to 50. The Skellam expectations are shown in dotted lines. The rapidity acceptance, $|y| < x$, is enlarged as x = 0.1, 0.2, ..., 0.5. The error bars are statistical and bands are systematic errors.

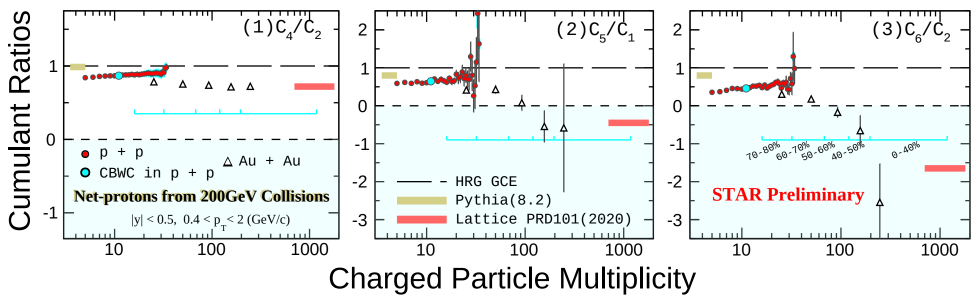

Figure 4: Charged hadron multiplicity dependence of the net-proton cumulant ratios, C_4/C_2, C_5/C_1, and C_6/C_2, from $\sqrt{s}$ = 200 GeV *p+p* (red circles) and Au+Au (triangles) collisions. Average values for *p+p* collisions are shown as light blue circles. Hadron resonance gas (HRG) model is shown as long-dashed lines. PYTHIA 8 and lattice QCD [6] calculations are shown as gold and red bands, respectively. The error bars are statistical errors. The corresponding centrality for Au+Au collisions are indicated as the light blue ticks.

6. Summary

Higher-order fluctuations of net-proton multiplicity distributions are measured for *p*+*p* collisions at $\sqrt{s}$ = 200 GeV. Cumulants and their ratios up to the sixth-order are presented, which are compared to results from Au+Au collisions. It is found that the cumulants increase with multiplicity and they have larger deviations from the Skellam and PYTHIA 8 calculations for higher-order cumulants. The rapidity acceptance dependence of cumulant ratios shows some deviations from the Skellam expectations and PYTHIA 8 calculations. The deviations become larger with increasing the acceptance. The multiplicity dependence of the cumulant ratios are compared between *p*+*p* and Au+Au collisions at $\sqrt{s_{\mathrm{NN}}}$ = 200 GeV. It is found that the C_5/C_1 and C_6/C_2 values are negative in Au+Au central collisions, while positive in *p*+*p* collisions at $\sqrt{s}$ = 200 GeV. Results for Au+Au collisions are progressively negative in more central collisions. The observations in Au+Au central collisions are qualitatively consistent with lattice QCD calculations, which could indicate a smooth crossover transition at top RHIC energy.

References

[1] Aoki, Y. et al., *the Order of the quantum chromodynamics transition predicted by the standard model of particle physic, Nature 443, 675 (2006) 675-678*

[2] Bowman, E. Scott and Kapusta, Joseph I., Critical Points in the Linear Sigma Model with Quarks, Phys. Rev. C 79 (2009) 015202 [arXiv:0810.0042].

[3] Adam, J. et al., Nonmonotonic Energy Dependence of Net-Proton Number Fluctuations, Phys. Rev. Lett. 126 (2021) 092301.

[4] Abdallah, M. S. et al., Cumulants and Correlation Functions of Net-proton, Proton and Antiproton Multiplicity Distributions in Au+Au Collisions at RHIC, Phys. Rev. C 104 (2021) 024902 [arXiv:2101.12413].

[5] Stephanov, M.A., On the sign of kurtosis near the QCD critical point, Phys. Rev. Lett. 107 (2011) 052301 [arXiv:1104.1627].

[6] Bazavov, A. et al., Skewness, kurtosis and the 5th and 6th order cumulants of net baryon-number distributions from lattice QCD confront high-statistics STAR data, Phys. Rev. D 101 (2020) 074502 [arXiv:2001.08530].

[7] Abdallah, M. S. et al., Measurement of the sixth-order cumulant of net-proton multiplicity distributions in Au+Au collisions at $\sqrt{s_{\mathrm{NN}}}$ *= 27, 54.4, and 200 GeV at RHIC, arXiv:2105.14698 (2021) [arXiv:2105.14698]*

[8] Bazavov, A. et al., The QCD Equation of State to $\mathcal{O}(\mu_B^6)$ *from Lattice QCD, Phys. Rev. D 95 (2017) 054504 [arXiv:1701.04325].*

[9] Nonaka, T. et al., More efficient formulas for efficiency correction of cumulants and effect of using averaged efficiency, Phys. Rev. C 95 (2017) 064912 [arXiv:1702.07106].

[10] Kitazawa, M. and Asakawa, M., Relation between baryon number fluctuations and experimentally observed proton number fluctuations in relativistic heavy ion collisions, Phys. Rev. C 86 (2012) 024904 [arXiv:1205.3292].

[11] Bzdak, A. and Koch, V., Acceptance corrections to net baryon and net charge cumulants, Phys. Rev. C 86 (2012) 044904 [arXiv:1206.4286].

[12] Nonaka, T. et al., Importance of separated efficiencies between positively and negatively charged particles for cumulant calculations, Phys. Rev. C 94 (2016) 034909 [arXiv:1604.06212].

[13] Bzdak, A. and Koch, V, Local Efficiency Corrections to Higher Order Cumulants, Phys. Rev. C 91 (2015) 027901 [arXiv:1312.4574].

[14] Luo, X., Unified Description of Efficiency Correction and Error Estimation for Moments of Conserved Quantities in Heavy-Ion Collisions, Phys. Rev. C 91 (2015) 034907 [arXiv:1410.3914].

[15] Luo, X. and Nonaka, T., Efficiency correction for cumulants of multiplicity distributions based on track-by-track efficiency, Phys. Rev. C 93 (2016) 044911 [arXiv:11602.01234].

[16] Kitazawa, M., Efficient formulas for efficiency correction of cumulants, Phys. Rev. C 99 (2019) 044917 [arXiv:1812.10303].

[17] Skokov, V. et al., Volume Fluctuations and Higher Order Cumulants of the Net Baryon Number, Phys. Rev. C 88 (2013) 034911 [arXiv:1205.4756].

[18] Luo, X. and Xu, N., Search for the QCD Critical Point with Fluctuations of Conserved Quantities in Relativistic Heavy-Ion Collisions at RHIC : An Overview, Nucl. Sci. Tech. 28 (2017) 112 [arXiv:1701.02105].